ELSEVIER

Journal of Physics and Chemistry of Solids 63 (2002) 545–554

JOURNAL OF PHYSICS AND CHEMISTRY OF SOLIDS

www.elsevier.com/locate/jpcs

Dynamics and crystal chemistry of tellurites 1. Raman spectra of thallium tellurites: Tl_2TeO_3, $Tl_2Te_2O_5$ and $Tl_2Te_3O_7$

A.P. Mirgorodsky, T. Merle-Méjean*, P. Thomas, J.-C. Champarnaud-Mesjard, B. Frit

Laboratoire de Science des Procédés Céramiques et de Traitements de Surface, UMR 6638 CNRS, Université de Limoges, Faculté des Sciences, 123, avenue Albert Thomas, 87060 Limoges Cedex, France.

Received 10 April 2001; accepted 10 July 2001

Abstract

Raman spectra of the three entitled crystals are analysed within the framework of a lattice-dynamical model treatment using preliminary obtained X-ray diffraction data. The short range atomic arrangement and spectrochemical peculiarities of these structures are jointly discussed, which is considered as an initial step for studying the nature of the glass phases in the $xTl_2O + (1 - x)TeO_2$ system. The charged TeO_3^{2-} groups and the neutral TeO_2 quasi-molecules are proposed as the basic units forming the complex tellurite anions. However, no relevant characteristic frequencies can be indicated in the spectra since the interatomic separation in those units are highly variables and their vibrational states are mixed and delocalised.

Keywords: D. Crystal structure

1. Introduction

Tellurites (Te IV) and the related compounds are rather promising materials for the optical device technology. They manifest good visible and infrared light transmittance, and have exceptionally high non-linear refractive index value n_2. Recent studies of TeO_2-based glasses have revealed that the latter value was the highest one found for oxide glasses and could be up to 100 times as large as that of SiO_2 [1,2]. This becomes the most pronounced when the modifiers contain elements having lone electron pairs (as example, for light wavelength 1.5 μm, the n_2 value of a commercial SiO_2 (Herasil) equals 0.12×10^{-19} m^2/W, and that for the 73.9mol%TeO_2–23.5mol%$TlO_{0.5}$–2.6mol% $BiO_{1.5}$ glass is about 9.1×10^{-19} m^2/W). The origin of those properties is of great interest for material science. Although its microscopic nature is still far from the final clarity, however, it is likely that it would directly relate to the peculiarities of the valence electron distribution, i.e. to the peculiarities in the short-range atomic arrangement.

This is one of the points due to which the tellurite structures can be considered among the most challenging objects of the modern physics and chemistry of solids. Actually, generally (if not always), they possess peculiarities mainly originating from the individual electron configuration of Te atoms involving a lone electron pair (E-pair). Because of the stereochemical activity of E-pairs, the Te–O chemical bonds are situated on one side of the Te atom, whereas the other side is a 'dead' zone of E-electrons which form 'empty' cavities of different shapes and volumes. Due to such a sharp asymmetry of the atomic arrangement of the first coordination spheres, the TeO_n polyhedra have strong dipole moments which provide considerable dipole–dipole contribution to the inter-anion potentials. This factor differentiates the energetics of the tellurium (IV)–oxygen systems from most of the other solid oxides.

The above mentioned features predispose the tellurite structures to be microscopically labile with respect to the cation–anion interactions, mechanically flexible with respect to the macroscopic strains, and very sensitive to

* Corresponding author. Tel.: +33-55-45-72-00; fax: +33-55-45-72-70.

E-mail address: merle@unilim.fr (T. Merle-Méjean).

0022-3697/02/$ - see front matter
PII: S0022-3697(01)00192-5

external electric fields, which displays itself in the extraordinary polarisation characteristics.

Thallium tellurites are compounds in which all the cations have E-pairs. Their crystal structures have complicated geometry and low symmetry. To our knowledge, the data on the vibrational spectra of thallium tellurite crystals are limited to that of Tl_2TeO_3 presented in Refs. [3,4] in the frame of a Raman study of several TeO_2-based glassy compounds. The vibrational properties of such crystals have never been discussed within the framework of a treatment including both aspects of the lattice dynamics and crystal chemistry. Little is known about the atomic arrangements in the relevant glasses, and their relations with the structural and chemical peculiarities of the crystals are not clear. In this situation, we have conducted a *comparative study of the vibrational and structural properties of crystals and glasses* for the $xTl_2O + (1 - x)TeO_2$ system.

In this paper, we present the Raman spectra of *all the crystalline phases found in that system*. We analyse them by using the results of the lattice-dynamical modelling jointly with the previously published X-ray diffraction (XRD) data on Tl_2TeO_3 [5], $Tl_2Te_2O_5$ [6] and $Tl_2Te_3O_7$ [7]. Methodologically, this can be regarded as a continuation of our preceding structural and spectrochemical studies of tellurium oxide polymorphs [8,9]. The properties of the related glasses and the mechanisms of their crystallisation will be discussed elsewhere [10].

2. Experimental

All the samples (Tl_2TeO_3, α-$Tl_2Te_2O_5$, β-$Tl_2Te_2O_5$, and $Tl_2Te_3O_7$) were prepared from various mixtures of high purity Tl_2CO_3 and TeO_2. The former was a commercial product (Aldrich, 99.9%). TeO_2 was prepared by decomposing commercial H_6TeO_6 (Aldrich, 99.9%) at 550°C. The synthesis process implied first heating (2°C/min) at 350°C for 18 h and then cooling down (2°C/min) at 250°C for 24 h the various mixtures in a gold crucible under pure flowing nitrogen. Well crystallised powder samples thus were obtained (with grain size in the range about 2–10 μ) and directly used for the Raman spectra recording. The latter was performed at ambient conditions in the 80–1200cm^{-1} range using a Dilor spectrometer (XY model) equipped with a CCD detector and an Ar^+ laser (514.5 nm exciting line) in a backscattering geometry. With such a detector, a good signal/noise ratio needed one or at most two scans (during 40–60 s). Several samples of each compound have been studied, and the spectra were repeatedly recorded from the different impact points of any sample. This was visually controlled through a microscope (×100), which had enabled us to analyse a surface with diameter of about 2 μm. The diameter of the laser spot focused on the sample was about 1 μm. Beautiful reproducibility of the results thus obtained was a proof of identity and homogeneity of the samples. Measurements were made at a low enough power (<100 mW) of the excitation line in order to avoid the destruction of the samples. The spectral resolution was about 4.5 cm^{-1} at the exciting line.

3. Crystal structure

In thoroughly studying the $xTl_2O–(1 - x)TeO_2$ system by XRD and Raman spectroscopy techniques, we have found four crystalline phases lying in the interval $0.5 \geq x > 0$. The crystal structures were definitively determined in our laboratory by X-ray single crystal diffraction methods for the three of them: Tl_2TeO_3 [5], α-$Tl_2Te_2O_5$ [6] and $Tl_2Te_3O_7$ [7]. For the fourth phase, β-$Tl_2Te_2O_5$, only the space group and the unit cell dimensions were determined [11]. The three former structures have been exhaustively characterised and all the experimental details relating to the XRD measurements were given in the original papers [5–7]. Therefore, only a brief description of those structures (necessary for the further discussion) are given below. Those structure are shown in Figs. 1–3, and some of their characteristics are given in Table 1.

Tl_2TeO_3 crystallises with the orthorhombic symmetry (space group: *Pban*-D_{2h}^4, unit cell parameters: $a = 16.60(1)$ Å, $b = 11.078(6)$ Å, $c = 5.238(8)$ Å, $Z = 8$). As mentioned above, due to the strong stereochemical activity of the lone pairs E, Te and Tl atoms have very asymmetric coordination polyhedra: $Tl(2)O_4$ disphenoids, $Tl(1)O_3$ and TeO_3 pyramids. By sharing either edges or corners, those polyhedra constitute Tl_2TeO_3 sheets along (010) between which the lone pairs E are located (Fig. 1a). Within those sheets, the coordination polyhedra of Te atoms can be considered as independent pyramidal ortho-anions $[TeO_3]^{2-}$ (Fig. 1b). The three nearly identical Te–O bonds (see Table 1) form O–Te–O angles of values 96.2, 98.0 and 98.2°. The 'dead' zone around the lone pair E of the Te atom involves three non-bonding Te···O contacts (3.06, 3.10 and 3.37 Å).

α-$Tl_2Te_2O_5$ has monoclinic symmetry (space group: $P2_1/n$-C_{2h}^5, unit cell parameters: $a = 7.119(1)$ Å, $b = 12.138(2)$ Å, $c = 8.439(2)$ Å, $\beta = 114.28(3)°$, $Z = 4$). All the atoms are in general positions 4c of the $P2_1/n$ space group. As in the Tl_2TeO_3 crystal structure, the distribution of oxygen atoms around each cation is highly anisotropic. For example, the shortest (1.8–2.4 Å) Te–O distances (Table 1) correspond to distorted disphenoids TeO_4 with the lone pair E forming the fifth equatorial corner of a TeO_4E trigonal bipyramid (Table 1 and Fig.2). By sharing O(1) and O(2) corners and O(3)–O(3) edges, those TeO_4 disphenoids constitute the Te_2O_5 two-dimensional network visualised in Fig. 2a. However, the Te(1)–O(3) and Te(2)–O(1) axial bonds with lengths of 2.16 and 2.33 Å, respectively, are clearly longer than the three other bonds of each TeO_4 disphenoid (see Table 1); so taking into account the preliminary considerations in Refs. [8,9]

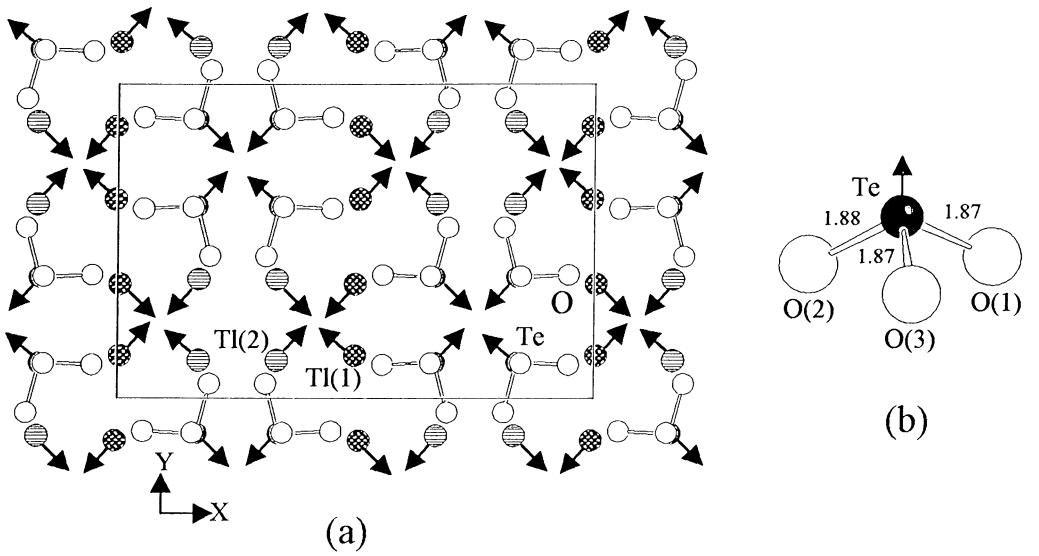

Fig. 1. (a) Projection onto (001) of the Tl_2TeO_3 crystal structure (arrows visualise the direction towards which are located the lone pairs E of Te and Tl atoms). (b) View of the independent pyramidal anion $[TeO_3]^{2-}$.

they can be regarded as electrostatic contacts separating the structural fragments shown in Fig 2b.

These fragments can be characterised as isolated diortho-anion $[Te_2O_5]^{2-}$. Whereas their four terminal bonds (1.870, 1.873, 1.908 and 1.925 Å) manifest a considerable asymmetry, the intra-anion Te(1)–O(2)–Te(2) bridge is quite 'balanced' (2.03 and 2.04 Å). We wish to underline that these bridges are formed by two axial bonds (Te–$_{ax}$O$_{ax}$–Te) which, to our knowledge, is a particular feature of the $[Te_2O_5]^{2-}$ diortho-anions. In α-$Tl_2Te_2O_5$, those complex anions are interrelated by the inversion symmetry operation, thus forming via the long Te(1)···O(3) contacts, so-called Te_2O_2 double bridges, similar to those observed in β-TeO_2 [12].

$Tl_2Te_3O_7$ crystallises with the triclinic symmetry (space group: P_1-C_i^1, unit cell parameters $a=$ 6.839(1) Å, $b=7.432(1)$ Å, $c=9.920(2)$ Å, $\alpha=$ 92.00 (3)°, $\beta=$ 108.95(3)°, $\gamma=112.85(3)°$, $Z=2$). The

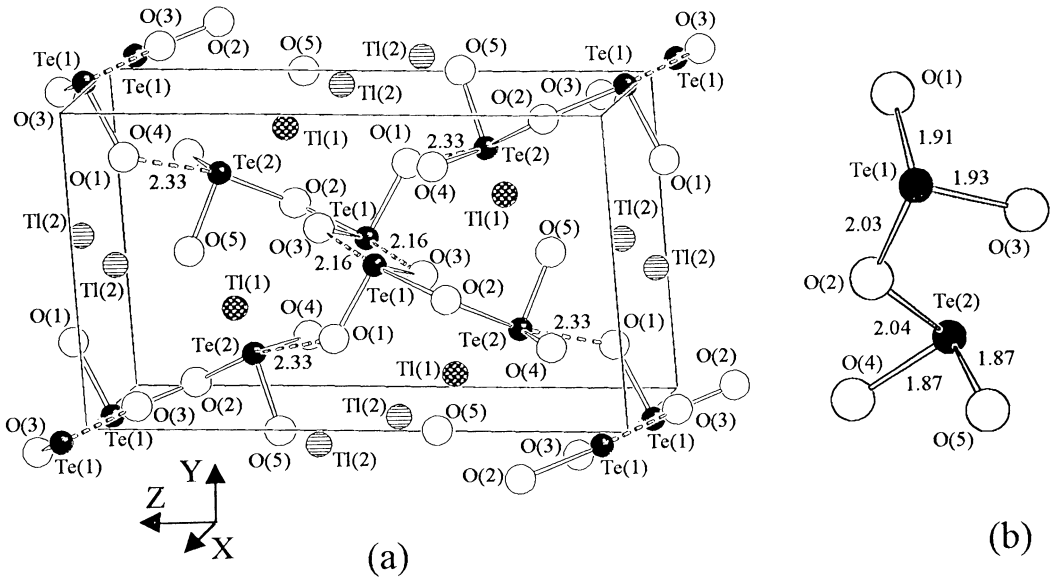

Fig. 2. The α-$Tl_2Te_2O_5$ crystal structure. (a) spatial view visualising the Te_2O_5 sheets parallel to (1 0 −1); (b) the $[Te(1)Te(2)O_5]^{2-}$ diortho-anion.

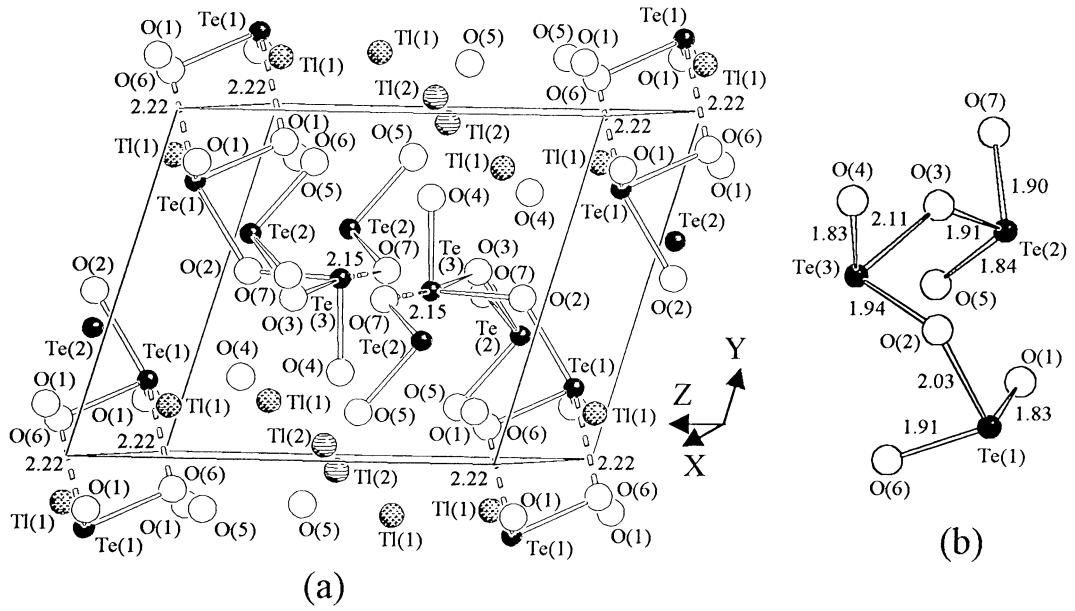

Fig. 3. The $Tl_2Te_3O_7$ crystal structure. (a) A perspective view; (b) the $[Te_3O_7]$ fragment.

inversion centre is a single nontrivial symmetry operation. All the atoms are in general 2i positions. Of the three crystallographically different tellurium atoms (Te(1), Te(2), and Te(3)), Te(2) is bonded to *three* oxygen atoms only (thus forming TeO_3 pyramid), whereas the Te(1), and Te(3) are summits of distorted disphenoids TeO_4. By sharing either edges ($Te(1)O_4$ polyhedra between them) or corners ($Te(3)O_4$ polyhedra with $Te(2)O_3$ pyramids on one side and $Te(1)O_4$ polyhedra on the other side), those polyhedra constitute highly corrugated strips extending infinitely along the *a* axis (Fig. 3a). However, the bond length criteria used above to specify the isolated $[Te_2O_5]^{2-}$ anions in the α-$Tl_2Te_2O_5$ crystal structure allow us to propose a three-fold coordination for the Te(1) and Te(2) atoms, since their fourth neighbours, O(6) and O(7), are distant from them by about 2.22 and 2.15 Å, respectively. Consequently, an independent complex anion $[Te_3O_7]^{2-}$ containing three TeO_3 polyhedra (Fig. 3b) can be isolated.

Its rather asymmetric configuration can be attributed to the anisotropy of the short-range anion–anion and overall cation–anion forces. Actually, the Te(1)–O(1) and Te(3)–O(7) potentials provide the strongest interactions between the complex anions (via the

$$\mathrm{Te(1)}\overset{\mathrm{O(1)}}{\underset{\mathrm{O(6)}}{\diamond}}\mathrm{Te(1)}$$

double bridges and the Te(3)···O(7) contacts respectively), which is not the case for the Te(2) atoms. Moreover, of the two oxygen atoms O(3) and O(2), forming the two intra-anion Te–O–Te bridges, the former is coordinated to a Tl atom, whereas the latter is not, so that the two Te–O(3) bridging bonds are more disparate (1.912 and 2.108 Å),

Table 1
Main tellurium-oxygen and thallium-oxygen distances in crystalline α-, β- and γ-TeO_2 and Tl-Te mixed oxides

Reference		Shortest Te–O distances (Å)	Shortest Tl–O distances (Å)
[17]	α-TeO_2	2.12 (×2); 1.88 (×2)	
[12]	β-TeO_2	1.87/1.89/2.07/2.15	
[8,9]	γ-TeO_2	1.858/1.945/2.022/2.202	
[7]	$Tl_2Te_3O_7$	Te(1): 1.833/1.912/2.032/2.223	Tl(1): 2.471/2.588/2.700/2.828
		Te(2): 1.837/1.898/1.912	Tl(2): 2.488/2.652/2.736/2.942
		Te(3): 1.834/1.943/2.108/2.154	
[6]	α-$Tl_2Te_2O_5$	Te(1): 1.908/1.925/2.034/2.162	Tl(1): 2.580/2.584/2.646/2.840
		Te(2): 1.870/1.873/2.041/2.327	Tl(2): 2.681/2.775/2.799/2.813
[5]	Tl_2TeO_3	1.868/1.871/1.877	Tl(1): 2.548/2.746/2.810
			Tl(2): 2.508/2.636/2.663/2.870

and their average length is longer than that of Te–O(2) ones (2.032 and 1.943 Å). As for the five non-bridging oxygen atoms, three of them are bonded to only one tellurium atom (the O(1), O(4) and O(5) atoms). Consequently the corresponding three terminal Te–O bonds (Te(1)–O(1), Te(2)–O(5), and Te(3)–O(4)) are the shortest and have lengths of about 1.83 Å which practically coincide with those observed in the isolated gaseous TeO_2 molecules [13].

The above lattices, Tl_2TeO_3, $Tl_2Te_2O_5$ and $Tl_2Te_3O_7$, characterise three points of the structural evolution of the $xTl_2O + (1-x)TeO_2$ system, for x varying from 0.5 to 0. The final point of this evolution is TeO_2, whose crystalline phases are traditionally described as three-dimensional networks built up from corner- or edge-sharing TeO_4 disphenoids [8,9].

Keeping this traditional point of view, it can be said that the decreasing x would drive the basic TeO_n polyhedra to change from a slightly distorted trigonal pyramid TeO_3 (distorted TeO_3E tetrahedron) to a TeO_4 disphenoid (TeO_4E trigonal bipyramid), via an intermediary TeO_{3+1} unit in which one of the two axial bonds (on average longer than the two equatorial ones) lengthens up to about 2.22–2.33 Å (see Table 1). At the same time, the degree of condensation of those TeO_n polyhedra would increase from isolated $[TeO_3]^{2-}$ ortho-anions to a three-dimensional network $(TeO_2)_\infty$, via isolated $[Te_2O_5]^{2-}$ and $[Te_3O_7]^{2-}$ complex anions.

4. Raman spectra and lattice dynamics

The Raman spectra for all the above mentioned thallium tellurite lattices are presented in Fig. 4. The high frequency bands between 600 and 800 cm^{-1} can be unambiguously attributed to the Te–O stretching vibrations, mainly corresponding to the motions of oxygen atoms, whereas the lowest parts of the spectra ($<200\ cm^{-1}$) can be associated with the motions of the heavy atoms Tl and Te. The origin of most of the bands in the interval 200–600 cm^{-1} is not so evident. To make the situation more transparent and informative, lattice dynamical calculations are necessary.

Such calculations have been conducted within the modified Valence Force Field Model in which the two-body short range Te–O, Tl–O and O–O interactions were taken into account jointly with the three-body interactions inside the O–Te–O and Te–O–Te bridges described via the diagonal bending force constants of these bridges and via the non-diagonal Te–O/Te–O force constants through atoms Te and O. The two-body constants were estimated from the empirically found dependences of the relevant force constants K on the interatomic distances (Fig. 5). The bending force constant values and those of the non-diagonal interactions were transferred from the lattice-dynamical model, earlier elaborated by us for the crystalline TeO_2 polymorphs [8,9].

The calculations were performed by using the code CRYME [14] expanded to the case of an arbitrary number of atoms per primitive cell. The values thus obtained were the frequencies ω of the longwave vibrations and their shapes (eigenvectors), the elastic constants C_{ik} and related values, and the derivatives $d\omega/dK$ and dC_{ik}/dK.

First, we can note in brief that according to the model estimations, the thallium tellurite crystals seem to be much more mechanically compliant than the condensed TeO_2 phases: their theoretical bulk moduli lie in the interval 10–12 GPa, whereas they are about 40 GPa for α- and β-TeO_2 [8]. This fact can be attributed to the weakness of the Tl–O potentials essentially contributing to the compression mechanism of the structures in question. However, the limits of this paper do not allow us to analyse all the calculation results, and we shall focus our attention on the consideration of the Raman-active vibrations.

The measured Raman spectrum of the **Tl_2TeO_3 crystal** in Fig. 4A is in good correspondence with the previous data of Refs. [3,4]. Since all the 48 atoms of the unit cell are in general positions, the 144 Brillouin zone centre normal coordinates are uniformly distributed between the eight irreducible representations of the D_{2h} group. Consequently, the longwave vibration spectrum of Tl_2TeO_3 ($144-3=141$ modes) has the following symmetry properties:

$$18\ A_g + 18\ B_{1g} + 18\ B_{2g} + 18\ B_{3g} + 18\ A_u + 17\ B_{1u} + 17\ B_{2u} + 17\ B_{3u}.$$

It is important to note that the island-like Tl_2TeO_3 crystal structure consists of independent and very heavy structural fragments: eight complex anions $[TeO_3]^{2-}$ and 16 cations Tl^+ per unit cell. Their relative motions are governed by forces corresponding to interatomic distances longer than 2.5 Å. Therefore, those forces are weak and the vibrations of those fragments as rigid units would be considerably softer than the 48 *internal* vibrations of the TeO_3 pyramids.

Correspondingly, of the 72 Raman-active calculated modes, 48 are situated below 200cm^{-1}. The 12 vibrations lying in the interval 280–350 cm^{-1} are chiefly related to the O–Te–O bending deformations of the TeO_3 pyramids. The most intense of them (near 290 cm^{-1}) corresponds to the A_g species. According to the calculations, the cation and rigid complex anion motions are essentially mixed, and it can be said that the strongest Tl–O forces (2.5–2.7 Å) mainly contribute to the modes between 120 and 200 cm^{-1}, whereas the lowest part of the spectrum is dominated by weak inter-pyramidal O–O interactions.

The 12 stretching vibrations of the Te–O bonds which occupy the interval 600–750 cm^{-1}, are worth closer examination. Actually, although the TeO_3 pyramid has the C_1 trivial symmetry, the Te–O bond lengths, as well as the values of the O–Te–O angles, do not differ drastically. Therefore, its three stretching and three bending vibrations can be described as the $A_1 + E$ ones in the symmetry terms of the C_{3v} pyramid-like molecule. According to the calculation, the group of highest frequency vibrations (700–725 cm^{-1}) (see Fig. 4A) corresponds to the stretching

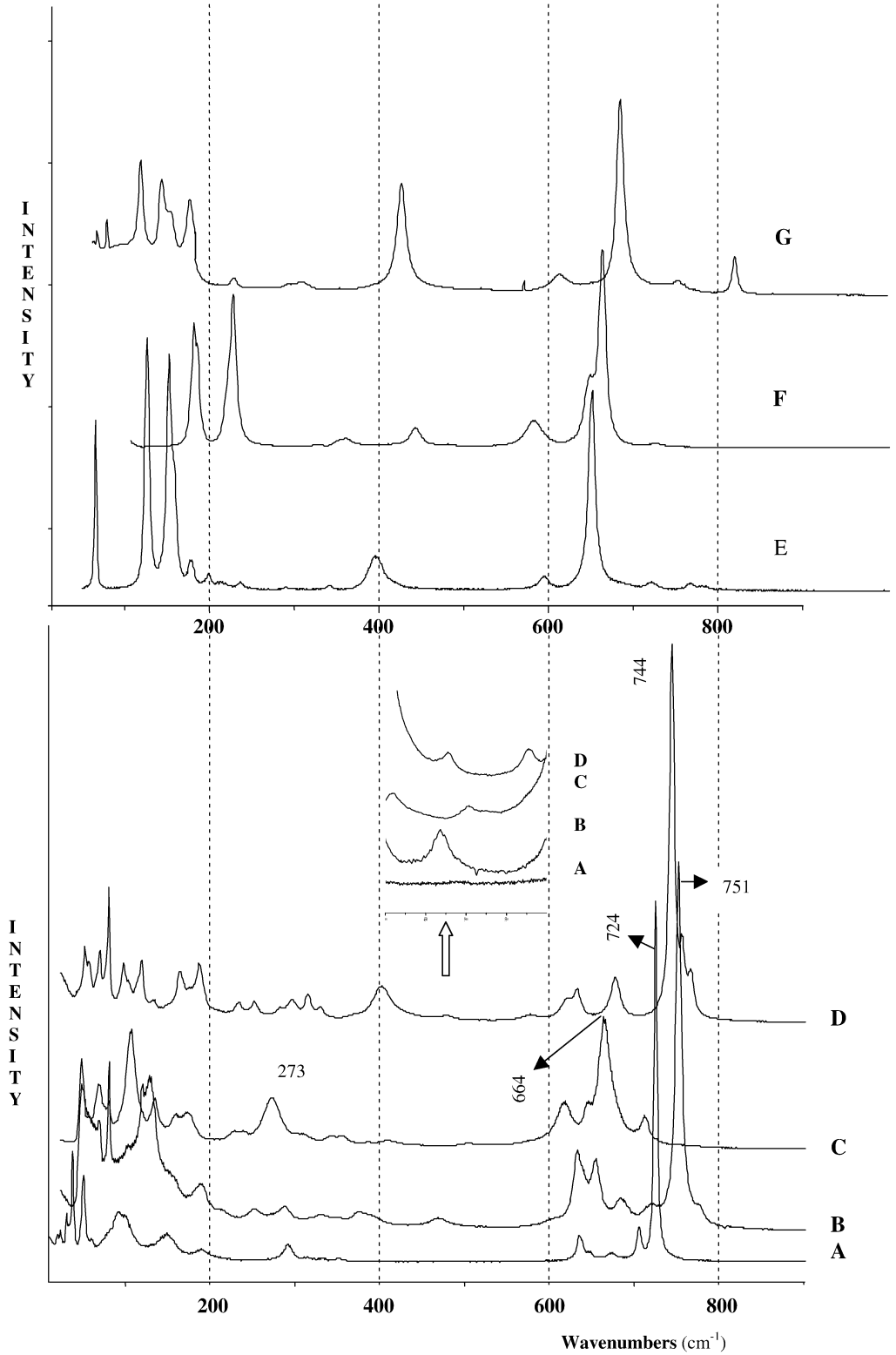

Fig. 4. Raman spectra of the thallium tellurites. (A) Tl_2TeO_3; (B) β-$Tl_2Te_2O_5$,; (C) α-$Tl_2Te_2O_5$,; (D) $Tl_2Te_3O_7$ and of the α- (E), β- (F) and γ-form (G) of TeO_2. The inset exhibits the details of 400–600 cm^{-1} range.

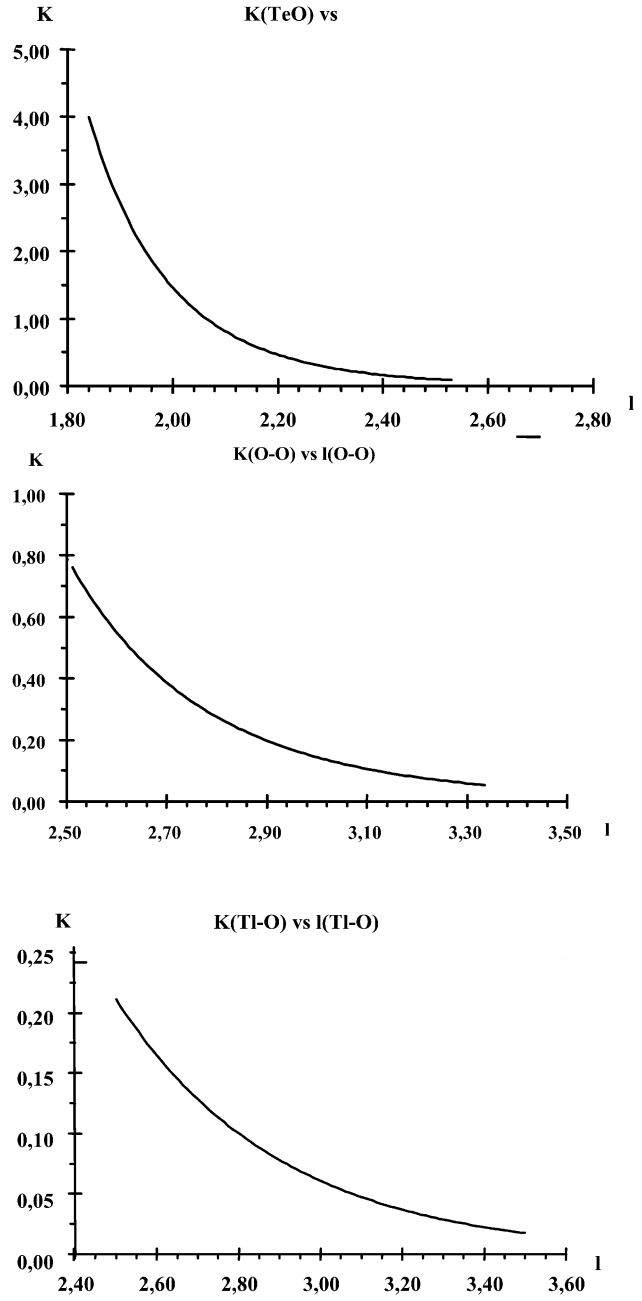

Fig. 5. Force constants K (mdyn/Å) versus bond lengths l (Å) for Te–O, O–O and Tl–O potentials (from top to bottom, respectively).

pulsations (A_1) of the TeO_3 pyramids. Their totally symmetric combination (A_g species) produces the strongest Raman band at 724 cm^{-1}. The other three combinations, B_{1g}, B_{2g}, and B_{3g} are practically not split and are situated near 705 cm^{-1}. The range 600–700 cm^{-1} contains the eight lines related to the E stretching motions of the TeO_3 pyramids.

The 105 longwave vibrations of the **α-$Tl_2Te_2O_5$ lattice** are distributed between the symmetry species as follows: 27 A_g + 27 B_g + 26 A_u + 25 B_u. The Raman spectrum of α-$Tl_2Te_2O_5$ contains fewer vibrations than that of Tl_2TeO_3 (see above), but in Fig. 4C it displays more lines since its structure has a less regular short range organisation, which favours the splitting of the vibrational modes. According to

the calculations, the vibrations forming the highest frequency part of the spectrum (600–720 cm^{-1}) are combinations of the stretching motions of the terminal Te–O bonds (1.870, 1.873, 1.908 and 1.925 Å). One of them, corresponding to the *synchronous motions* (but with different amplitudes) of those bonds, produces the strongest line near 664 cm^{-1}.

The *asymmetric stretching vibrations* of the intra-anion Te–$_{ax}$O$_{ax}$–Te bridges have very weak intensity, and lie near 500 cm^{-1} (exceptionally low, in our opinion), whereas the *symmetric* ones can be associated with the intense band near 273 cm^{-1}. The symmetric vibrations of the $Te(1)_2O_2$ double bridges are situated near 410 cm^{-1}, slightly lower than for their homologue in β-TeO_2 [8]. The bands in the interval 200–400 cm^{-1} mainly originate from the deformations of the O–Te–O angles, and the region below 200 cm^{-1} can be attributed to the motions of the heavy structural fragments (as in the spectrum of Tl_2TeO_3).

The Raman spectrum of the metastable β-form of $Tl_2Te_2O_5$ is shown in Fig. 4B. Since the detailed crystal structure is still unknown, no serious analysis of this spectrum can be done. However, it is likely that the position of the strongest line (751 cm^{-1}) indicates the presence in this structure of rather short terminal bonds.

The 69 longwave vibrations of **$Tl_2Te_3O_7$** lattice belong to the two symmetry species, 36 A_{g+} 33 A_u. Most of the Raman-active modes (36 A_g) seems to be seen in Fig. 4D. According to the calculations, the high-frequency part of the spectrum (600–800 cm^{-1}) can be interpreted in terms of the stretching vibrations of the $[Te_3O_7]^{2-}$ fragment, containing nine Te–O bonds. Five of them with lengths in the range 1.83–1.91 Å (see Table 1 and Fig. 3) are terminal ones. The four remaining bonds form the *intra-anion* Te–O–Te bridges via oxygen atoms O(3) (1.912–2.108 Å) and O(2) (1.943–2.032 Å). The calculations show that the highest frequency band (740–770 cm^{-1}) in Fig. 4D mainly originates from the vibrations of seven bonds: the above mentioned five *terminal* Te–O bonds and the two shortest bridging ones (Te(2)–O(3) = 1.912 Å and Te(3)–O(2) = 1.94 Å). The strongest peak in that band can be associated with the synchronous stretchings of all those bonds. The region 400–600 cm^{-1} can be mainly associated with the Te–O–Te bridge vibrations. The lower-frequency part of the spectrum, like in the above considered cases, can be attributed to the deformations of the complex anions and to their motions jointly with Tl^+ cations.

5. Discussion

According to the lattice-dynamical modelling of the Raman spectra of thallium tellurite lattices, the bands above 200 cm^{-1} in Fig. 4A–D can be reliably associated with the internal deformations of the complex anions.

We will first concentrate on the highest-frequency modes (600–800 cm^{-1}). The calculations show that the *most intense* of them can be associated with the *synchronous stretching motions* of the Te–O bonds shorter than 1.95 Å. Some of those bonds contribute to the Te–$_{ax}$O$_{eq}$–Te bridges, and their vibrations can be formally regarded as the asymmetric ones of such bridges. However, if these bridges had been built from *pairs* of covalent bonds, their asymmetric vibrations could not be strong in the Raman spectra (this point is discussed in detail in Ref. [8]). Therefore, the strong Raman intensities observed for the highest-frequency part of the spectra in Fig. 4A–D indicate that the relevant bands relate to the vibrations of the essentially *terminal* bonds. Thus, from the spectrochemical point of view, all the Te–O_{eq} bonds should be considered as *terminal* ones. This means that the Te–$_{ax}$O$_{eq}$–Te linkages in the $Tl_2Te_2O_5$ and $Tl_2Te_3O_7$ crystals contain only *one* covalent bond (Te–O_{eq}), and the Te–O_{ax} contacts cannot be attributed to this category.

Firstly, such an issue allows us to recognise the Te_2O_5 and Te_3O_7 groups in those two crystals as the isolated structural fragments previously determined in Sec. II by using the bond-length criteria. So the spectrochemical characteristics of the high-frequency atomic vibrations of the thallium tellurites support the point of view according to which the Te–O_{ax} 'bonds' (longer than the sum of the covalent radii of O and Te) should be considered as electrostatic contacts.

The existence of such contacts seems to be natural (and sometime even inevitable) for the tellurites and condensed TeO_2 crystal structures. Actually, any asymmetric (polar) TeO_n polyhedron would necessarily have positive (Te) and negative (O) extremities. The oppositely charged extremities of the neighbouring polyhedra would attract each other, thus forming *inter-polyhedron* Te···O contacts longer than 2.0 Å, which minimise the electrostatic (dipole–dipole) energy of the lattice. It is interesting to note that the so-called Te_2O_2 double bridges (i.e, the parallelepipeds in which two opposite edges are short Te–O bonds, and the other two edges are the Te···O contacts), as a rule, have *inversion symmetry,* thus indicating an anti-parallel orientation of the dipole moments of the neighbouring units, i.e. the largely electrostatic character of their interactions.

Secondly, the following question arises: is our above conclusion about the absence of the Te–O–Te covalent bonding in $Tl_2Te_2O_5$ and $Tl_2Te_3O_7$ consistent with other vibrational properties of these structures?

Therefore, we focus on the middle-frequency range (400–600 cm^{-1}). Actually, the Raman spectra of ionic-covalent crystalline oxides having the X–O–X bridges manifest in this range a very strong band (if this is permitted by rules of symmetry) associated with the *symmetric* stretching vibrations of such bridges. (A classic example of this is the spectra of SiO_2 polymorphs (see Ref. [8] for references).) A high Raman intensity is inherent for these sorts of vibrations (see Section 4 in Ref. [8]).

We wish to recall now that the structural evolution of our

system from Tl_2TeO_3 to TeO_2 corresponds to an increasing condensation of the TeO_n polyhedra from the isolated $[TeO_3]^{2-}$ ortho-anions to the $[TeO_2]_\infty$ networks of the TeO_2 polymorphs. Due to this, the number of the Te–O–Te fragments inside the complex anions would also increase. Consequently, on average, the intensity of the middle frequency Raman lines would increase. Such a general tendency can be seen in Fig. 4 (compare the spectrum of Tl_2TeO_3 consisting of isolated ortho-anions to that of γ-TeO_2 containing polymerised Te–O–Te chains).

At the same time, no *strong bands are present* in the interval 400–600 cm^{-1} in the spectra of the $Tl_2Te_2O_5$ and $Tl_2Te_3O_7$ crystals (Fig. 4B–D) in which the symmetric vibrations of the covalent Te–O–Te bridges had to lie [8,9] (similar to a strong band near 430 cm^{-1} in Fig. 4G). Thus, one more time, the spectrochemical evidence indicates the absence of the Te–O–Te covalent bridges in those crystals. So, it can be concluded that the condensation of the TeO_n polyhedra into the complex thallium tellurite anions is not associated with their polymerisation (i.e. with the formation of the Te–O–Te covalent bridges).

We have already analysed such a phenomenon in the frame of a lattice-dynamical treatment of the TeO_2 lattices [8,9]. Traditionally the α- and β-TeO_2 polymorphs are considered as three-dimensional networks of TeO_4 disphenoids sharing only corners in α-TeO_2 and both corners and edges in β-TeO_2 [12,15]. Each TeO_4 disphenoid contains two equatorial bonds (2×1.88 Å in α-TeO_2, 1.87 and 1.89 Å in β-TeO_2) and two axial bonds (2×2.12 Å in α-TeO_2, 2.07 and 2.15 Å in β-TeO_2) which form the single or double dissymetric Te–$_{eq}O_{ax}$–Te bridges. Such a definition of the coordination polyhedra around Te atoms is usually argued by the electrostatic estimations of the bond valence values [16].

Another point of view comes from the lattice-dynamical treatment of these two crystal structures [8,9]. Actually, from the spectrochemical position, the difference between the equatorial and the axial Te–O bonds is so important that the existence of isolated TeO_2^{eq} 'pseudo-molecules' (interconnected via electrostatic Te···O_{ax} contacts) in α-TeO_2 and β-TeO_2 is more pronounced than the Te–$_{eq}O_{ax}$–Te three-dimensional polymerisation. Such an issue is not something new. It just argues for the previously proposed opinion that paratellurite (α-TeO_2) could be regarded as a molecular crystal (see Ref. [17] and references therein) rather than a three-dimensional network.

At the same time, for the new metastable form γ-TeO_2 [8,9] in which half of the Te–O_{ax} bonds shorten (in comparison with the values in the α- and β-polymorphs) to about 2.0 Å and half lengthen up to 2.2 Å, a well pronounced effect of a one-dimensional Te–$_{eq}O_{ax}$–Te polymerisation can be seen in the Raman spectrum (Fig. 4G). This allowed us to consider the γ-TeO_2 crystal structure as a chain structure (like crystalline SeO_2) in which each Te atom is three-coordinated at the apex of a distorted TeO_3 trigonal pyramid.

Keeping in mind the above mentioned results, we will concentrate now on the questions: (a) how do the TeO_n polyhedra change during the structural evolution of our system from Tl_2TeO_3 to TeO_2? (b) What are the elementary units forming the Te_2O_5 and Te_3O_7 isolated anions, and how are those units interconnected? (c) How is the valence electron distribution arranged within the complex tellurite anions?

According to the point of view implying the molecular nature of the α- and β-form of TeO_2, the question (a) could be readily answered: 'they evolve from the charged $[TeO_3]^{2-}$ group to the neutral TeO_2 quasi-molecule'. Under the *former* term, we shall understand the TeO_3 pyramid with three short Te–O bonds of about 1.83–1.93 Å; and the *latter* term will correspond to the TeO_4 disphenoid, similar to those present in the α- and β-TeO_2 crystal structures, in which *two* O atoms form the Te–O_{eq} bonds with lengths around 1.86–1.90 Å, and the two O_{ax} atoms are separated from Te by about 2.10 Å and more.

Answering question (b), it can be said that the structural units forming the complex tellurite anions are: (i) the $[TeO_3]^{2-}$ pyramids; (ii) the TeO_2 quasi-molecules; and (iii) the $[Te_2O_5]^{2-}$ groups which can be regarded either as diortho-anions (i.e. two adjusted TeO_3 pyramids sharing one corner) or as two TeO_2 pseudo-molecules keeping between them an O^{2-} anion ($TeO_2 + O^{2-} + TeO_2$). In the complex tellurite anions, these three types of units can coexist being mutually linked by Te···O potentials similar to those which keep together the 'pseudo-molecules' in α- and β-TeO_2 crystals.

In connection with question (c), we venture the hypothesis that there are the following charge–structure correlations for such units: (i) the higher the TeO_3 group is charged, the more it resembles the isolated $[TeO_3]^{2-}$ ortho-anion and vice versa (this seems to be in line with the quantum chemistry calculations [18]); and (ii) the closer to zero the charge of the TeO_n polyhedron, the more its atomic arrangement corresponds to the TeO_2 quasi-molecule.

By looking at the $[Te_3O_7]^{2-}$ complex anion in Fig. 3b, we can note that only the Te(2) atom unequivocally forms a TeO_3 group. Thus, according to the above hypothesis, this group would concentrate the most part of the anion charge. Therefore, we could *conventionally* decompose the $[Te_3O_7]^{2-}$ anion as the sum of the three units: $[TeO_3]^{2-} + TeO_2 + TeO_2$, in relating the first unit with atom Te(2), and the two TeO_2 pseudo-molecules with the Te(1) and Te(3) atoms. Such an interpretation is in agreement with the model analysis of the vibrational spectrum of $Tl_2Te_3O_7$: as was noticed in Section 3, the strongest line in Fig. 4D (near 744 cm^{-1}) can be associated with the *synchronous* stretching motions of the *seven* Te–O bonds forming the above three units. In the same way, it is possible to assume that, as an alternative to the Te_2O_5 diortho-group, the $[Te_2O_5]^{2-}$ anion could exist as the $[TeO_3]^{2-} + TeO_2$ combination; it may be that this situation is realised in β-$Tl_2Te_2O_5$, the band at 751 cm^{-1} in Fig. 4B corresponding then to the pulsation of the TeO_3 pyramid. In such a case, the

Te–O bond lengths can be estimated to be about 1.85 Å and shorter. It is interesting to note that differently charged complex anions as $[Te_5O_{11}]^{2-}$ and $[Te_3O_8]^{4-}$ in lead tellurites [19,20] or $[Te_4O_{11}]^{6-}$ in chromium [21] and gallium [22] tellurites can be regarded as various combinations of the elementary structural units $[TeO_3]^{2-}$ and TeO_2.

Evidently, the proposed scheme is rather simplified, but it seems to be capable of drawing the main trends of the charge distribution inside the complex tellurite anions, and of the 'structure–charge' correlation for the tellurium–oxygen coordination spheres.

6. Concluding remarks

By using lattice-dynamical and spectrochemical arguments, we propose an interpretation of the structural and chemical peculiarities of thallium tellurites, which differs from the traditional description of the tellurium-oxygen systems. Within the framework of this approach, the tellurite (IV) anions (with exceptions for the mixed TeIV-TeVI oxides in which the coordination of tellurium atoms can be rather particular [23]) are regarded as consisting of *two types* of basic structural units: the *charged* $[TeO_3]^{2-}$ groups; and the *neutral* TeO_2 quasi-molecules. Theoretically, it suggests that in the general case, the 'quasi-molecular' tellurium dioxide in reacting with a modifier can provide the tellurite structures in which some TeO_2 molecules are transformed into the charged TeO_3 units, and some molecules remain in the initial (neutral) state. Although this approach is schematic and simplified, it allows us to clarify the main tendency in a *non-homogeneous* distribution of the valence electron charge within the complex tellurite anions.

Thus, it can be said, that, unlike such traditional glass-former complex oxides as silicates, germanates, phosphates, etc., in which the XO_4 units vary their charges, but always (independently of cations) keep the tetrahedron geometry (and thus keep the characteristic peculiarities in their vibrational spectra), in the tellurite anions, *both* charges and atomic arrangements of the structural polyhedra are essentially variable. Consequently, it is likely that the high frequency *stretching vibration* spectra of the tellurites (the most informative from the point of view of the crystal chemistry) have not any conservative features typical for a given structural type of the tellurite anions, and can be considered as personalised characteristics of their short-range atomic arrangements very sensitive to the inter-ion interactions.

Acknowledgements

One of the authors (A.P.M.) participated in this work in quality of invited researcher of the CNRS of France. He thanks Professor J.F. Baumard, director of Laboratory SPCTS, for the invitation and for interest in this work.

References

[1] S.H. Kim, T. Yoko, S. Sakka, J. Am. Ceram. Soc. 76 (1993) 1061.
[2] B. Jeansannetas, S. Blanchandin, P. Thomas, P. Marchet, J.C. Champarnaud-Mesjard, T. Merle-Méjean, B. Frit, V. Nazabal, E. Fargin, G. Le Flem, M.O. Martin, B. Bousquet, L. Canioni, S. Le Boiteux, P. Segonds, L. Sarger, J. Sol. State Chem. 146 (1999) 329.
[3] J. Dexpert-Ghys, B. Piriou, S. Rossignol, J.M. Reau, B. Tanguy, J.J. Videau, J. Portier, J. Non-Cryst. Solids 170 (1994) 167.
[4] T. Sekiya, N. Mochida, A. Ohtsuka, M. Tonokawa, J. Non-Cryst. Solids 144 (1992) 128.
[5] B. Frit, D. Mercurio, P. Thomas, J.-C. Champarnaud-Mesjard, Z. Kristallogr. 214 (1999) 439.
[6] P. Thomas, B. Jeansannetas, P. Marchet, J.C. Champarnaud-Mesjard, B. Frit, Mat. Res. Bull. 33 (1998) 1709.
[7] B. Jeansannetas, P. Thomas, J.-C. Champarnaud-Mesjard, B. Frit, Mat. Res. Bull. 32 (1997) 51.
[8] A.P. Mirgorodsky, T. Merle-Méjean, J.-C. Champarnaud-Mesjard, P. Thomas, B. Frit, J. Phys. Chem. Solids 61 (2000) 501.
[9] J.-C. Champarnaud-Mesjard, S. Blanchandin, P. Thomas, A.P. Mirgorodsky, T. Merle-Méjean, B. Frit, J.Phys.Chem. Solids 61 (2000) 1499.
[10] T. Merle-Méjean, A.P. Mirgorodsky, J.-C. Champarnaud-Mesjard, P. Thomas, B. Frit, (to be published).
[11] B. Jeansannetas, Thesis, University of Limoges, 1998.
[12] V.H. Beyer, Z. Kristallogr. 124 (1967) 228.
[13] D.W. Muenov, J.W. Hastie, R. Hauge, Trans. Faraday Soc. 65 (1969) 3210.
[14] M.B. Smirnov, A.P. Mirgorodsky, P.E. Quintard, J. Mol. Structure 348 (1995) 159.
[15] O. Lindquist, Acta Chem. Scan. 22 (1968) 977.
[16] I.D. Brown, J. Solid State Chem. 11 (1974) 214.
[17] P.A. Thomas, J. Phys. C: Solid State Phys. 21 (1988) 4611.
[18] S. Suehara, S. Hishita, S. Inoue, A. Nukui, Phys. Rev. B 58 (1998) 14124.
[19] A. Oufkir, M. Dutreilh, P. Thomas, J.-C. Champarnaud-Mesjard, P. Marchet, B. Frit, Mat. Res. Bull. 36 (2001) 693.
[20] J.C. Devan, A.J. Edwards, G.R. Jones, I.M. Young, J.C.S. Dalton (1978) 1528.
[21] G. Meunier, J. Frit, J. Galy, Acta Cryst. B32 (1976) 175.
[22] M. Dutreilh, P. Thomas, J.C. Champarnaud-Mesjard, B. Frit, Solid State Sciences 3 (2001) 423.
[23] I. Alves Weil, Thesis, University of Bordeaux I (France), 2000.